HHS Public Access

Author manuscript

Eur J Neurosci. Author manuscript; available in PMC 2023 January 01.

Published in final edited form as:

Eur J Neurosci. 2022 January ; 55(1): 264–276. doi:10.1111/ejn.15512.

Microstructural white matter abnormalities in Lesch–Nyhan disease

Victor A. Del Bene[1,2], **Jeffrey L. Crawford**[1], **Ainara Gómez-Gastiasoro**[3], **Tracy D. Vannorsdall**[1,4], **Alison Buchholz**[1], **Natalia Ojeda**[2], **James C. Harris**[1,†], **Hyder A. Jinnah**[5], **David J. Schretlen**[1,6]

[1]Department of Psychiatry and Behavioral Sciences, The Johns Hopkins University School of Medicine, Baltimore, Maryland, USA

[2]Department of Neurology, University of Alabama at Birmingham, Birmingham, Alabama, USA

[3]Department of Methods and Experimental Psychology, University of Deusto, Bilbao, Spain

[4]Department of Neurology, The Johns Hopkins University School of Medicine, Baltimore, Maryland, USA

[5]Departments of Neurology and Human Genetics, Emory University School of Medicine, Atlanta, Georgia, USA

[6]Russell M. Morgan Department of Radiology and Radiological Science, The Johns Hopkins University School of Medicine, Baltimore, Maryland, USA

Abstract

Lesch–Nyhan disease is a rare, sex-linked, genetic neurodevelopmental disorder that is characterized by hyperuricemia, dystonia, cognitive impairment and recurrent self-injury. We previously found reduced brain white matter volume in patients with Lesch–Nyhan disease compared with healthy adults using voxel-based morphometry. Here, we address the structural integrity of white matter via diffusion tensor imaging. We hypothesized that white matter integrity would be decreased in men with Lesch–Nyhan disease and to a lesser extent in men with a milder variant of the disease (Lesch–Nyhan variant) relative to healthy men. After acquiring diffusion-weighted brain images from Lesch–Nyhan disease ($n = 5$), Lesch–Nyhan variant ($n = 6$) and healthy participants ($n = 10$), we used both tract-based spatial statistics and a regions of

Correspondence: David J. Schretlen, Department of Psychiatry and Behavioral Sciences, The Johns Hopkins University School of Medicine, 600 North Wolfe Street, Meyer 218, Baltimore, MA 21287, USA. dschret@jhmi.edu.
Present address: Jeffrey L. Crawford, Department of Psychology at the University of Connecticut in Storrs, Connecticut, USA
†Died April 5, 2021

AUTHOR CONTRIBUTIONS

DJS, HAJ and JCH were involved in the study design. TDV and AB collected the data. VDB, JLC and AGG analysed the data. Data interpretation was completed by DJS, VDB, JLC, AGG and HAJ. VDB wrote the initial draft of the manuscript with DJS, JLC, TDV, AB, NO, JCH and HAJ also contributing to the writing. Figures were created by JLC and AGG. Funding was secured by DJS and HAJ.

CONFLICT OF INTEREST

We declare no conflicts of interest.

PEER REVIEW

The peer review history for this article is available at https://publons.com/publon/10.1111/ejn.15512.

SUPPORTING INFORMATION

Additional supporting information may be found in the online version of the article at the publisher's website.

interest approach to analyse between-group fractional anisotropy differences. We first replicated earlier findings of reduced intracranial, grey matter and white matter volumes in patients. We then discovered marked reductions of fractional anisotropy relative to the healthy control group. The Lesch–Nyhan disease group showed more pronounced reductions in white matter integrity than the Lesch–Nyhan variant group. In addition to whole brain fractional anisotropy group differences, reductions in white matter integrity were observed in the corpus callosum, corona radiata, cingulum, internal capsule and superior longitudinal fasciculus. Moreover, the variant group had attenuated dystonia severity symptoms and cognitive deficits. These findings high-light the need to better understand the role of white matter in Lesch–Nyhan disease.

Keywords

cognition; diffusion tensor imaging; Lesch–Nyhan disease; Lesch–Nyhan variant; magnetic resonance imaging; white matter

1 | INTRODUCTION

Lesch–Nyhan disease (LND) is a rare, sex-linked, genetic disorder of purine metabolism that leads to a characteristic neurodevelopmental phenotype (Harris, 2018; Torres & Puig, 2007). It occurs almost exclusively in males, and the phenotype consists of hyperuricemia, severe dystonia, cognitive impairment and recurrent self-injury (Anderson & Ernst, 1994; Jinnah et al., 2006, 2010; Nyhan, 1976). LND is caused by mutations of the *HPRT1* gene found on the X chromosome long-arm (q26–q27) (Fu et al., 2013), which encodes the purine salvage enzyme, hypoxanthine-guanine phosphoribosyltransferase (HPRT) (Fu et al., 2013; Nguyen et al., 2017). Residual HPRT of less than 1.5% typically produces classic LND. Partial HPRT deficiencies between 1.5% and 20% produce an attenuated phenotype variant (Lesch–Nyhan variant [LNV]) (Fu et al., 2013, 2014). Persons with LNV typically show less severe abnormalities than those with LND, and they do not self-injure (Jinnah et al., 2010).

Research has primarily focused on the basal ganglia and dopaminergic dysfunction in LND (Ceballos-Picot et al., 2009; Göttle et al., 2014; Jinnah et al., 1999; Lloyd et al., 1981; Nyhan, 2000; Saito & Takashima, 2000; Wong et al., 1996), with aberrant metabolic uptake on positron emission tomography (PET) imaging in the basal ganglia, frontal cortex and midbrain (Ernst et al., 1996). Patients have reduced basal ganglia volumes (Schretlen et al., 2013), as well as PET evidence for abnormal dopamine fibres in the basal ganglia (Ernst et al., 1996). Compared with the relatively extensive research into contributions of the basal ganglia and dopaminergic pathways to LND, much less is known about the possible contribution of brain white matter (WM) abnormalities. Using voxel-based morphometry (VBM), we previously found that adults with LND showed a 17% reduction in brain grey matter (GM) and 26% reduction of WM volumes relative to healthy controls (HC) (Schretlen et al., 2015). WM matter volume reductions were prominent in the inferior frontal and medial inferior regions of the brain. Moreover, evidence from mouse models suggest that axon and dendrite are impoverished in LND and that along with myelin, WM is mostly comprised of these neurites with HPRT deficiency resulting in aberrant arborization (Mikolaenko et al., 2005) and growth during the cell differentiation process

(Guibinga et al., 2010). Neurites require purines for energy, and it is more economical to recycle purines via HPRT than it is to produce de novo purines (Mikolaenko et al., 2005). The altered development of neurites has also been observed in models of autism, Fragile X syndrome, Down syndrome, and movement disorders, such as Huntington's disease (Fiala et al., 2002; Gilbert & Man, 2017; Guidetti et al., 2001; Jagadha & Becker, 1989). Therefore, these findings raise the question of whether reduced WM volume and integrity contributes to the LND phenotype. Diffusion tensor imaging (DTI) enables one to measure the microstructural integrity of WM fibre tracts (Le Bihan et al., 2001), unlike the VBM methodology previously used by our group (Schretlen et al., 2015). Because volume and integrity reflect different anatomical properties, it is possible that WM abnormalities in LND extend beyond the loss of volume to include a more fundamental disruption of the structural integrity of affected brain pathways, such as altered and impoverished arborization due to impaired HPRT functioning. Based on prior findings (Mikolaenko et al., 2005; Schretlen et al., 2015), we hypothesized that patients with LND and LNV would show decreased WM integrity compared with HC and that this would be greater in LND than LNV.

2 | MATERIALS AND METHODS

2.1 | Participants and procedure

Twenty-four participants had T1-weighted and diffusion-weighted brain MRI scans. They included 7 men with LND, 7 men with LNV, and 10 healthy men as control participants (HC). One person with LND was excluded from the volumetric analysis because his T1-weighted images could not be segmented due to motion artefact, although his diffusion-weighted scan was viable and included in the DTI analysis.

Classic LND was diagnosed based on a history of hyperuricemia, self-injurious behaviour, cognitive impairment and motor neurological abnormalities. Fibroblast assays confirmed the diagnosis by showing residual HPRT enzyme activity less than 1.6% of normal or a mutation in the *HPRT1* gene that predicted null enzyme activity. Participants with LNV were diagnosed if they had overproduction of uric acid but not self-injury. The diagnosis was confirmed by evidence of residual HPRT enzyme greater than 1.5% of normal, an *HPRT1* gene mutation, or both. Data collection took place between 2009 and 2013. All patients were recruited through our clinics, other physicians, the Lesch–Nyhan Disease Patient Registry, and the Matheny School and Hospital in Peapack, New Jersey, USA. When possible, all participants gave written informed consent to participate in the study. Otherwise, written informed consent was obtained from a legal guardian of the patient, and the patient gave oral assent to participate. Healthy participants were recruited from the local community and were part of the Bipolar and Schizophrenia Network for Intermediate Phenotypes (BSNIP) consortium study. Exclusion criteria for the HC group included a history of neurological disorders, substance abuse or dependence, or psychiatric illness. This study was approved by the Johns Hopkins Medicine and Emory University institutional review boards and was conducted in accordance with the Declaration of Helsinki. Data are available online https://github.com/JeffCrawford/Microstructural-White-Matter-Abnormalities-in-Lesch-Nyhan-Disease_article

2.2 | Image acquisition and processing

T1-weighted and diffusion-weighted brain scans were acquired for all the participants using a Siemens Magnetom TrioTim (3 T). T1-weighted image parameters were TR = 2300 ms; TE = 2.9 ms; FOV = 256 mm; flip angle = 9°; voxel size = 1.0 × 1.0 × 1.2 mm. Diffusion-weighted images were obtained using a single-shot spin-echo planar imaging (EPI) with a twice-refocused balance echo sequence. Image parameters for most of the participants were TR = 6700 ms; TE = 92 ms; FOV = 1610 × 1610 mm; voxel size = 1.8 × 1.8 × 3.0 mm; *b* value = 1000 s/mm^2; 48 slices. Thirty diffusion directions were acquired for all the participants. However, two HC had a different TR (6900 and 7100 ms), FOV (1840 × 1840 mm) and number of slices (50 and 51). The difference was due to a change in the BSNIP protocol in the early stages. These two participants were retained to match for age. In addition, a software update took place during theacquisition period. Therefore, acquisition sequence was included as a covariate in DTI analyses. At least two exact repetitions of the diffusion-weighted sequence were acquired due to expected movement artefacts. All patients with classic LND and some with LNV were given alprazolam (.5–1.0 mg per 23 kg) to limit movement artefact.

Total intracranial, cortical GM, subcortical GM and WM volumes were obtained using automated volumetric measurement with FreeSurfer. The cortical GM volume consists of volumes obtained specifically from the cortex and the subcortical GM volume consists of the following bilateral volumes: thalamus, caudate, putamen, pallidum, hippocampus, amygdala, nucleus accumbens and ventral diencephalon. The segmentation was done using FreeSurfer v6 (https://surfer.nmr.mgh.harvard.edu/) on a Windows 7 computer with a VMware virtual machine using a CentOS 6 Linux operating system. All FreeSurfer derived volumes were imported into SPSS 24 software for statistical analyses.

Diffusion images were processed using FSL version 6 (https://fsl.fmrib.ox.ac.uk/fsl/fslwiki). FSL's Brain Extraction Tool (BET) (Smith, 2002) was used to remove non-brain tissue. Eddy was used to correct for distortions and movement. We also used the eddy FSL function to identify volumes with excessive absolute or relative motion. Using the Kruskal–Wallis *H* test, no significant differences were found between groups when assessing mean motion values ($p = .327$). However, FSL's Quality Assessment for DMRI (QUAD) and Study-wise Quality Assessment for DMRI (SQUAD) (Bastiani et al., 2019) identified three participants (LND = 2, LNV = 1) with excessive movement. Removing these participants from the DTI analysis yielded a final sample of five LND participants, six LNV participants, and ten HC. Fractional anisotropy (FA) maps were generated using DTIFIT tool, implemented in the FMRIB's diffusion toolbox (Behrens et al., 2003).

2.3 | Statistical analyses

Individual data for clinical and cognitive scores, brain MRI volumes and whole brain FA values are provided in Tables 1 and 2. Clinical and cognitive scales include the Burke–Fahn–Marsden Dystonia Rating Scale (BFM) (Fahn et al., 1998), Kaufman Brief Intelligence Test—Second Edition (KBIT2) (Kaufman, 2004), Hopkins Verbal Learning Test—Revised (HVLT-R) (Brandt, 1991), Brief Test of Attention (BTA) (Schretlen et al., 1996) and Benton Facial Recognition Test (BFRT) (Benton et al., 1994). Except for the IQ measure (KBIT2,

standard score, $M = 100$, $SD = 15$), only raw scores for clinical and cognitive measures (i.e., not demographically adjusted) are presented in Table 1. Pairwise comparisons for clinical and cognitive data and structural brain MRI volumes (total intracranial volume, cortical and subcortical volumes, and WM volume) were completed by calculating Hedges' g (Table 3), rather than using inferential statistics and relying on p values, which has the potential for misinterpretation (Wetzels et al., 2011), particularly in a small sample. Additional subcortical volumes are also reported in Table 2. MRI volumes and the FA values for regions of interest are also depicted as scatter plots (MatLab R2019b) to more clearly visualize the data (Rousselet et al., 2016).

FSL's tract-based spatial statistics (TBSS) was used to analyse FA group differences. All participant FA maps were first aligned to one another with the 'most representative' map identified and used as the target image. Then, the target image was affine-aligned to a common MNI152 space (tbss_2_reg -n) using a non-linear transformation, and every other participant's FA map were then transformed to 1 × 1 × 1 mm MNI152 standard space (tbss_3_postreg -S). This approach was selected, rather than the standard approach of using the FMRIB58_FA standard space, because the brains of people with LND are smaller in volume on average. Next, all FA maps were merged into a single 4D image file. The mean FA skeleton was created using a threshold of .2, with the skeleton representing the centres of all tracts common to the group.

FA comparisons were performed between (a) 11 patients (5 LND plus 6 LNV) vs. 10 HC, (b) 5 LND patients vs. 10 HC and (c) 5 LND patients vs. 6 LNV patients. These comparisons were tested using Randomise (5000 permutations) (Winkler et al., 2014), a non-parametric permutation analysis tool. Total intracranial volume, age and acquisition sequence were included as covariates in all DTI analyses. Significant clusters were identified using the threshold free cluster enhancement (TFCE) (Smith & Nichols, 2009), and all TBSS analyses were corrected for family-wise error (FWE-corrected). For visualization purposes, only unthresholded FA images are presented (Allen et al., 2012), whereas significant clusters in the tables were thresholded with significance levels and cluster size provided to help organize the WM tracts where group differences were observed. Significant regions were located and labelled anatomically with the *MRI Atlas of Human White Matter* (Oishi et al., 2010). Following TBSS analysis, we extracted each participant's whole brain FA value, and then used the JHU DTI-based white-matter atlas (Mori et al., 2005) to isolate bilateral regions of interest in the cingulum, genu, body, and splenium of the corpus callosum (CC), internal capsule, including anterior and posterior portions of the internal capsule, and the superior longitudinal fasciculus. This was done to further explore and characterize possible WM integrity differences between the groups given the small sample size of our study.

3 | RESULTS

3.1 | Clinical and cognitive variables

Regarding clinical variables (Table 1), both LND and LNV groups had substantially lower IQ estimates (KBIT2), as well as notable deficits on tests of attention (BTA), facial recognition (BFRT), and both auditory-verbal learning (HVLT-R L) and delayed memory

recall (HVLT-R D). Cognitive deficits were most notable in the LND group with the level of impairment attenuated in the LNV group. Similarly, LND participants had a greater dystonia severity and the LNV participants had milder dystonia symptom severity.

3.2 | MRI volumes

Broadly, both LND and LNV participants have reduced total intracranial, cortical, subcortical and WM volumes relative to the HC group (Tables 2 and 3, Figure 1). When comparing LND and LNV groups, WM volume was notably reduced in the LND group (Tables 2 and 3). Additional subcortical brain region volumes are also presented in Table 2.

3.3 | Whole brain differences in WM integrity

With respect to the TBSS Randomise analysis, compared with HC, the combined patient group (LND + LNV) did not differ in terms of WM integrity. However, compared with HC, the patients with LND showed reduced WM integrity in the genu and body of the CC, as well as the bilateral anterior corona radiata (Table 4; Figure 2). No group differences were observed when contrasting LNV and HC participants. In addition, patients with LND showed reduced WM integrity compared with those with LNV in the CC, cingulum and superior corona radiata of the left hemisphere, although corresponding reductions in the right hemisphere did not reach statistical significance (Table 5; Figure 3).

With respect to group region of interest differences, FA comparisons and Hedges' g values are presented in Table 6 and shown in Figures 4 and 5. Although the TBSS analysis did not reveal WM integrity differences between HC and the combined LND and LNV participants, the region of interest analyses revealed that the combined clinical group had reduced WM integrity in multiple regions, including the whole brain, cingulum, anterior limb of the internal capsule, superior longitudinal fasciculus, and the genu and body of the CC. Comparing LND with healthy participants, the largest differences in WM integrity involve whole brain FA, cingulum, internal capsule, anterior limb of the internal capsule, superior longitudinal fasciculus, and the genu, body, and splenium of the CC. The LNV participants showed reduced WM integrity relative to HC participants in the cingulum, with marginal differences at the whole brain level, anterior limb of the internal capsule, and in the body of the CC, although the direction was reversed in the internal capsule and posterior limb of the internal capsule. There were large FA differences in the whole brain, cingulum, internal capsule, anterior limb of the internal capsule, superior longitudinal fasciculus, and the CC between the LNV and LND group, with the latter consistently showing reduced WM integrity. Finally, the LND and LNV groups showed greater WM integrity than HC in the posterior limb of the internal capsule.

4 | DISCUSSION

The results of the current study revealed widespread GM and WM abnormalities in LND and LNV. First, using a different volumetric segmentation methodology from our prior study in a subset of participants who were all scanned on a single 3 Tesla machine, we replicated our previous findings of reduced total intracranial, cortical and subcortical GM, and WM volumes in patients with LND and LNV (Schretlen et al., 2013). We then, for the first

time, demonstrated atypical WM integrity in LND patients using both TBSS and region of interest approaches. We further found that patients with LNV and LNV differ in their WM integrity. Past research that reported widespread WM volume reductions in LND patients led to speculation that there also might be underlying abnormal WM integrity (Schretlen et al., 2015). As hypothesized, we found WM integrity reductions in classic LND patients relative to healthy adults. These reductions affect multiple major intra-hemispheric and interhemispheric WM fibres tracts. These findings suggest that persons with LND, and to a lesser extent LNV, have reduced WM integrity between cortical and subcortical regions, which contributes to the phenotype.

This study provides the first evidence of reduced WM integrity in LND and extends our knowledge of the disorder, by providing further evidence that WM volume and integrity should be considered in LND and LNV models. Because no degenerative changes are apparent in autopsy studies (Göttle et al., 2014), the reductions of WM volumes and integrity likely result from altered neural development, such as disrupted development of neurites that partially comprise WM (Mikolaenko et al., 2005). Although LND is not typically considered a WM disorder, it seems likely that WM abnormalities contribute to the neurological and behavioural phenotype, with further research needed to confirm our findings.

The relationship between spasticity and the corticospinal tract is well documented (Brown, 1994; Mukherjee & Chakravarty, 2010). In a study of 44 LND patients, the most prominent motor sign was dystonia, but 23% of LND patients also demonstrated spasticity, along with other corticospinal tract signs such as clonus, extensor toe reflex and pathological brisk muscle stretch reflexes (Jinnah et al., 2006). Spasticity in this population may result from diminished connectivity from the motor cortex, and we therefore anticipated that the WM integrity of the posterior limb of the internal capsule would be reduced in the LND group. However, the observed pattern was in the opposite direction. Given the small sample size of our three groups, it is difficult to know if this is a region where LND and LNV participants truly do not have reduced WM integrity, or if reductions would have been observed in a larger sample that better approximates a normal distribution. Further investigation with a larger sample size is warranted as this finding is not consistent with the clinical phenotype.

The regions of WM where integrity is reduced could relate to the phenotype characteristics that distinguish LND and LNV. Abnormalities of the CC are associated with intellectual abilities (Luders et al., 2007). In addition, individuals with agenesis of the CC show deficits in reasoning, problem solving and social cognition (Brown & Paul, 2000). Reduced WM integrity of the cingulum is associated with deficits in attention (Kim et al., 2006) and obsessive–compulsive behaviours (Milad & Rauch, 2012). The cingulum is also associated with pain (Fuchs et al., 1996) and cognitive control and responds to environmental demands (Metzler-Baddeley et al., 2012). Self-injury is a cardinal feature of LND, and electrically stimulating the cingulum can induce rats to engage in self-injurious behaviours (Pellicer et al., 1999; Vaccarino & Melzack, 1991). Dysfunction of the pathways responsible for motivation has been proposed as an explanation for the recurrent self-harm seen in LND (Visser et al., 2000). Increasing our understanding of self-harm in LND patients could

illuminate shared neural mechanisms of self-injury in other patient populations and perhaps offer clues to effective intervention for such behaviours.

One limitation of the study is our small sample size. This mainly reflects the rarity of LND, although several participants had a DTI scanner-related artefact (Gallichan et al., 2010) that was not discovered until after we began data collection and rendered their diffusion-weighted scans unusable, and another three were excluded due to excessive head movements. This limited our ability to use inferential statistics and our statistical power to identify WM tract abnormalities using TBSS while correcting for multiple comparisons. Finally, had we acquired data with more directions and a second higher *b* value, we could have potentially modelled our data with greater sophistication, although the parameters used were consistent with the acquisition parameters commonly used at the time of study design. Because LND/LNV is an ultra-rare disease and the study is complete, it is unfortunately not feasible to obtain more data at this point. Nonetheless, this study represents the largest (and only) sample of LND/LNV patients in which WM integrity has been investigated using DTI. Future research will be needed to elucidate the relationship of the integrity of these WM tracts with behaviour, cognition and affect, perhaps via tractography of projections emanating from the basal ganglia or histopathological studies.

5 | CONCLUSION

Relative to the HC group, LND participants showed reduced WM integrity, and both clinical groups have reduced WM volume, cortical and subcortical GM volumes. Moreover, both clinical groups had elevated symptoms of dystonia and notable cognitive deficits. Whether on cognitive and clinical measures, or observed on various neuroimaging metrics, the LND group had the greatest disease burden and more pronounced volumetric and WM differences, whereas the LNV sample had more attenuated declines. This is the first DTI study of people with LND/LNV. The results demonstrated reductions of WM integrity, including whole brain FA, the CC, corona radiata, cingulum, internal capsule and superior longitudinal fasciculus. These findings highlight the importance of further studying WM in LND and LNV to better understand the relationship of WM with the cognitive, motor and behavioural phenotype. Additionally, it might be possible to glean information about self-harm through studying WM in LND (e.g., cingulum) and how this may overlap with other neurological and psychiatric disorders where self-harm is a clinical symptom.

Supplementary Material

Refer to Web version on PubMed Central for supplementary material.

ACKNOWLEDGEMENT

This study was supported by the National Institute of Child Health and Human Development (RO1 HD053312), the National Institute of Neurological Disorders and Stroke (NS109242) and the National Center for Advancing Translational Sciences (TR001456).

Funding information

National Institute of Neurological Disorders and Stroke, Grant/Award Numbers: NH1009242, NS109242; National Center for Advancing Translational Sciences, Grant/Award Number: TR001456; National Institute of Child Health and Human Development, Grant/Award Number: RO1 HD053312

DATA AVAILABILITY STATEMENT

Neuroimaging data are available for download from https://github.com/JeffCrawford/Microstructural-White-Matter-Abnormalities-in-Lesch-Nyhan-Disease_article.

Abbreviations:

BFM	Burke–Fahn–Marsden Dystonia Rating Scale
BFRT	Benton Facial Recognition Test
BTA	Brief Test of Attention
DTI	diffusion tensor imaging
FA	fractional anisotropy
GM	grey matter
HC	healthy control
HPRT	hypoxanthine-guanine phosphoribosyltransferase
HVLT-R	Hopkins Verbal Learning Test—Revised
IQ	intelligence quotient
KBIT2	Kaufman Brief Intelligence Test—Second Edition
LND	Lesch–Nyhan disease
LNV	Lesch–Nyhan variant
MRI	magnetic resonance imaging
VBM	voxel-based morphometry
WM	white matter.

REFERENCES

Allen EA, Erhardt EB, & Calhoun VD (2012). Data visualization in the neurosciences: Overcoming the curse of dimensionality. Neuron, 74, 603–608. 10.1016/j.neuron.2012.05.001 [PubMed: 22632718]

Anderson LT, & Ernst M (1994). Self-injury in Lesch-Nyhan disease. Journal of Autism and Developmental Disorders, 24, 67–81. 10.1007/BF02172213 [PubMed: 8188575]

Bastiani M, Cottaar M, Fitzgibbon SP, Suri S, Alfaro-Almagro F, Sotiropoulos SN, Jbabdi S, & Andersson JL (2019). Automated quality control for within and between studies diffusion MRI data using a non-parametric framework for movement and distortion correction. NeuroImage, 184, 801–812. 10.1016/j.neuroimage.2018.09.073 [PubMed: 30267859]

Behrens TE, Woolrich MW, Jenkinson M, Johansen-Berg H, Nunes RG, Clare S, Matthews PM, Brady JM, & Smith SM (2003). Characterization and propagation of uncertainty in diffusion-weighted MR imaging. Magnetic Resonance in Medicine: An Official Journal of the International Society for Magnetic Resonance in Medicine, 50, 1077–1088. 10.1002/mrm.10609

Benton AL, Abigail B, Sivan AB, Hamsher K.d., Varney NR, & Spreen O (1994). Contributions to neuropsychological assessment: A clinical manual Oxford University Press.

Brandt J (1991). The Hopkins Verbal Learning Test: Development of a new memory test with six equivalent forms. The Clinical Neuropsychologist, 5, 125–142. 10.1080/13854049108403297

Brown P (1994). Pathophysiology of spasticity. Journal of Neurology, Neurosurgery, and Psychiatry, 57, 773–777. 10.1136/jnnp57.7.773 [PubMed: 8021658]

Brown WS, & Paul LK (2000). Cognitive and psychosocial deficits in agenesis of the corpus callosum with normal intelligence. Cognitive Neuropsychiatry, 5, 135–157. 10.1080/135468000395781

Ceballos-Picot I, Mockel L, Potier M-C, Dauphinot L, Shirley TL, Torero-Ibad R, Fuchs J, & Jinnah H (2009). Hypoxanthine-guanine phosphoribosyl transferase regulates early developmental programming of dopamine neurons: Implications for Lesch-Nyhan disease pathogenesis. Human Molecular Genetics, 18, 2317–2327. 10.1093/hmg/ddp164 [PubMed: 19342420]

Ernst M, Zametkin AJ, Matochik JA, Pascualvaca D, Jons PH, Hardy K, Hankerson JG, Doudet DJ, & Cohen RM (1996). Presynaptic dopaminergic deficits in Lesch–Nyhan disease. New England Journal of Medicine, 334, 1568–1572. 10.1056/NEJM199606133342403 [PubMed: 8628337]

Fahn S, Bressman S, & Marsden C (1998). Classification of dystonia. Advances in Neurology, 78, 1–10.

Fiala JC, Spacek J, & Harris KM (2002). Dendritic spine pathology: Cause or consequence of neurological disorders? Brain Research Reviews, 39, 29–54. 10.1016/S0165-0173(02)00158-3 [PubMed: 12086707]

Fu R, Ceballos-Picot I, Torres RJ, Larovere LE, Yamada Y, Nguyen KV, Hegde M, Visser JE, Schretlen DJ, & Nyhan WL (2013). Genotype–phenotype correlations in neurogenetics: Lesch-Nyhan disease as a model disorder. Brain, 137, 1282–1303. 10.1093/brain/awt202 [PubMed: 23975452]

Fu R, Chen C-J, & Jinnah H (2014). Genotypic and phenotypic spectrum in attenuated variants of Lesch–Nyhan disease. Molecular Genetics and Metabolism, 112, 280–285. 10.1016/j.ymgme.2014.05.012 [PubMed: 24930028]

Fuchs PN, Balinsky M, & Melzack R (1996). Electrical stimulation of the cingulum bundle and surrounding cortical tissue reduces formalin-test pain in the rat. Brain Research, 743, 116–123. 10.1016/S0006-8993(96)01035-9 [PubMed: 9017238]

Gallichan D, Scholz J, Bartsch A, Behrens TE, Robson MD, & Miller KL (2010). Addressing a systematic vibration artifact in diffusion-weighted MRI. Human Brain Mapping, 31, 193–202. 10.1002/hbm.20856 [PubMed: 19603408]

Gilbert J, & Man H-Y (2017). Fundamental elements in autism: From neurogenesis and neurite growth to synaptic plasticity. Frontiers in Cellular Neuroscience, 11, 359. 10.3389/fncel.2017.00359 [PubMed: 29209173]

Göttle M, Prudente CN, Fu R, Sutcliffe D, Pang H, Cooper D, Veledar E, Glass JD, Gearing M, & Visser JE (2014). Loss of dopamine phenotype among midbrain neurons in Lesch–Nyhan disease. Annals of Neurology, 76, 95–107. 10.1002/ana.24191 [PubMed: 24891139]

Guibinga G-H, Hsu S, & Friedmann T (2010). Deficiency of the housekeeping gene hypoxanthine–guanine phosphoribosyltransferase (hprt) dysregulates neurogenesis. Molecular Therapy, 18, 54–62. 10.1038/mt.2009.178 [PubMed: 19672249]

Guidetti P, Charles V, Chen E-Y, Reddy PH, Kordower JH, Whetsell WO Jr., Schwarcz R, & Tagle DA (2001). Early degenerative changes in transgenic mice expressing mutant huntingtin involve dendritic abnormalities but no impairment of mitochondrial energy production. Experimental Neurology, 169, 340–350. 10.1006/exnr.2000.7626 [PubMed: 11358447]

Harris JC (2018). Lesch–Nyhan syndrome and its variants: Examining the behavioral and neurocognitive phenotype. Current Opinion in Psychiatry, 31, 96–102. 10.1097/YCO.0000000000000388 [PubMed: 29227296]

Jagadha V, & Becker LE (1989). Dendritic pathology: An overview of Golgi studies in man. Canadian Journal of Neurological Sciences, 16, 41–50. 10.1017/S0317167100028493

Jinnah H, Ceballos-Picot I, Torres RJ, Visser JE, Schretlen DJ, Verdu A, Larovere LE, Chen C-J, Cossu A, & Wu C-H (2010). Attenuated variants of Lesch-Nyhan disease. Brain, 133, 671–689. 10.1093/brain/awq013 [PubMed: 20176575]

Jinnah H, Jones M, Wojcik B, Rothstein J, Hess E, Friedmann T, & Breese G (1999). Influence of age and strain on striatal dopamine loss in a genetic mouse model of Lesch-Nyhan disease. Journal of Neurochemistry, 72, 225–229. 10.1046/j.1471-4159.1999.0720225.x [PubMed: 9886073]

Jinnah H, Visser JE, Harris JC, Verdu A, Larovere L, Ceballos-Picot I, Gonzalez-Alegre P, Neychev V, Torres RJ, & Dulac O (2006). Delineation of the motor disorder of Lesch–Nyhan disease. Brain, 129, 1201–1217. 10.1093/brain/awl056 [PubMed: 16549399]

Kaufman AS (2004). Kaufman brief intelligence test–second edition (KBIT-2) American Guidance Service.

Kim SJ, Jeong D-U, Sim ME, Bae SC, Chung A, Kim MJ, Chang KH, Ryu J, Renshaw PF, & Lyoo IK (2006). Asymmetrically altered integrity of cingulum bundle in posttraumatic stress disorder. Neuropsychobiology, 54, 120–125. 10.1159/000098262 [PubMed: 17199097]

Le Bihan D, Mangin JF, Poupon C, Clark CA, Pappata S, Molko N, & Chabriat H (2001). Diffusion tensor imaging: Concepts and applications. Journal of Magnetic Resonance Imaging: An Official Journal of the International Society for Magnetic Resonance in Medicine, 13, 534–546. 10.1002/jmri.1076

Lloyd KG, Hornykiewicz O, Davidson L, Shannak K, Farley I, Goldstein M, Shibuya M, Kelley WN, & Fox IH (1981). Biochemical evidence of dysfunction of brain neurotransmitters in the Lesch-Nyhan syndrome. New England Journal of Medicine, 305, 1106–1111. 10.1056/NEJM198111053051902 [PubMed: 6117011]

Luders E, Narr KL, Bilder RM, Thompson PM, Szeszko PR, Hamilton L, & Toga AW (2007). Positive correlations between corpus callosum thickness and intelligence. NeuroImage, 37, 1457–1464. 10.1016/j.neuroimage.2007.06.028 [PubMed: 17689267]

Metzler-Baddeley C, Jones DK, Steventon J, Westacott L, Aggleton JP, & O'Sullivan MJ (2012). Cingulum microstructure predicts cognitive control in older age and mild cognitive impairment. Journal of Neuroscience, 32, 17612–17619. 10.1523/JNEUROSCI.3299-12.2012 [PubMed: 23223284]

Mikolaenko I, Rao LM, Roberts RC, Kolb B, & Jinnah H (2005). A Golgi study of neuronal architecture in a genetic mouse model for Lesch–Nyhan disease. Neurobiology of Disease, 20, 479–490. 10.1016/j.nbd.2005.04.005 [PubMed: 15908225]

Milad MR, & Rauch SL (2012). Obsessive-compulsive disorder: Beyond segregated cortico-striatal pathways. Trends in Cognitive Sciences, 16, 43–51. 10.1016/j.tics.2011.11.003 [PubMed: 22138231]

Mori S, Wakana S, Van Zijil CM, & Nagae-Poetscher LM (2005). MRI Atlas of Human White Matter Elsevier, Amsterdam, The Netherlands.

Mukherjee A, & Chakravarty A (2010). Spasticity mechanisms—For the clinician. Frontiers in Neurology, 1. 10.3389/fneuro.2010.00149

Nguyen KV, Naviaux RK, & Nyhan WL (2017). Novel mutation in the human HPRT1 gene and the Lesch-Nyhan disease. Nucleosides, Nucleotides and Nucleic Acids, 36, 704–711. 10.1080/15257770.2017.1395037

Nyhan WL (1976). Behavior in the Lesch-Nyhan syndrome. Journal of Autism and Childhood Schizophrenia, 6, 235–252. 10.1007/BF01543464 [PubMed: 1086851]

Nyhan WL (2000). Dopamine function in Lesch-Nyhan disease. Environmental Health Perspectives, 108, 409–411. 10.1289/ehp.00108s3409 [PubMed: 10852837]

Oishi K, Faria AV, van Zijl PC, & Mori S (2010). MRI Atlas of Human White Matter Academic Press.

Pellicer F, López-Avila A, & Torres-López E (1999). Electric stimulation of the cingulum bundle precipitates onset of autotomy induced by inflammation in rat. European Journal of Pain, 3, 287–293. 10.1016/S1090-3801(99)90056-3 [PubMed: 10700357]

Rousselet GA, Foxe JJ, & Bolam JP (2016). A few simple steps to improve the description of group results in neuroscience. European Journal of Neuroscience, 44, 2647–2651. 10.1111/ejn.13400 [PubMed: 27628462]

Saito Y, & Takashima S (2000). Neurotransmitter changes in the pathophysiology of Lesch–Nyhan syndrome. Brain and Development, 22, 122–131. 10.1016/S0387-7604(00)00143-1

Schretlen D, Bobholz JH, & Brandt J (1996). Development and psychometric properties of the Brief Test of Attention. The Clinical Neuropsychologist, 10, 80–89. 10.1080/13854049608406666

Schretlen DJ, Varvaris M, Ho TE, Vannorsdall TD, Gordon B, Harris JC, & Jinnah H (2013). Regional brain volume abnormalities in Lesch-Nyhan disease and its variants: A cross-sectional study. The Lancet Neurology, 12, 1151–1158. 10.1016/S1474-4422(13)70238-2 [PubMed: 24383089]

Schretlen DJ, Varvaris M, Vannorsdall TD, Gordon B, Harris JC, & Jinnah H (2015). Brain white matter volume abnormalities in Lesch-Nyhan disease and its variants. Neurology, 84, 190–196. 10.1212/WNL.0000000000001128 [PubMed: 25503620]

Smith SM (2002). Fast robust automated brain extraction. Human Brain Mapping, 17, 143–155. 10.1002/hbm.10062 [PubMed: 12391568]

Smith SM, & Nichols TE (2009). Threshold-free cluster enhancement: Addressing problems of smoothing, threshold dependence and localisation in cluster inference. NeuroImage, 44, 83–98. 10.1016/j.neuroimage.2008.03.061 [PubMed: 18501637]

Torres RJ, & Puig JG (2007). Hypoxanthine-guanine phosophoribosyltransferase (HPRT) deficiency: Lesch-Nyhan syndrome. Orphanet Journal of Rare Diseases, 2, 48. 10.1186/1750-1172-2-48 [PubMed: 18067674]

Vaccarino AL, & Melzack R (1991). The role of the cingulum bundle in self-mutilation following peripheral neurectomy in the rat. Experimental Neurology, 111, 131–134. 10.1016/0014-4886(91)90060-P [PubMed: 1984429]

Visser J, Baer P, & Jinnah H (2000). Lesch–Nyhan disease and the basal ganglia. Brain Research Reviews, 32, 449–475. 10.1016/S0165-0173(99)00094-6 [PubMed: 10760551]

Wetzels R, Matzke D, Lee MD, Rouder JN, Iverson GJ, & Wagenmakers E-J (2011). Statistical evidence in experimental psychology: An empirical comparison using 855 t tests. Perspectives on Psychological Science, 6, 291–298. 10.1177/1745691611406923 [PubMed: 26168519]

Winkler AM, Ridgway GR, Webster MA, Smith SM, & Nichols TE (2014). Permutation inference for the general linear model. NeuroImage, 92, 381–397. 10.1016/j.neuroimage/2014.01.060 [PubMed: 24530839]

Wong DF, Harris JC, Naidu S, Yokoi F, Marenco S, Dannals RF, Ravert HT, Yaster M, Evans A, & Rousset O (1996). Dopamine transporters are markedly reduced in Lesch-Nyhan disease in vivo. Proceedings of the National Academy of Sciences, 93, 5539–5543. 10.1073/pnas.93.11.5539

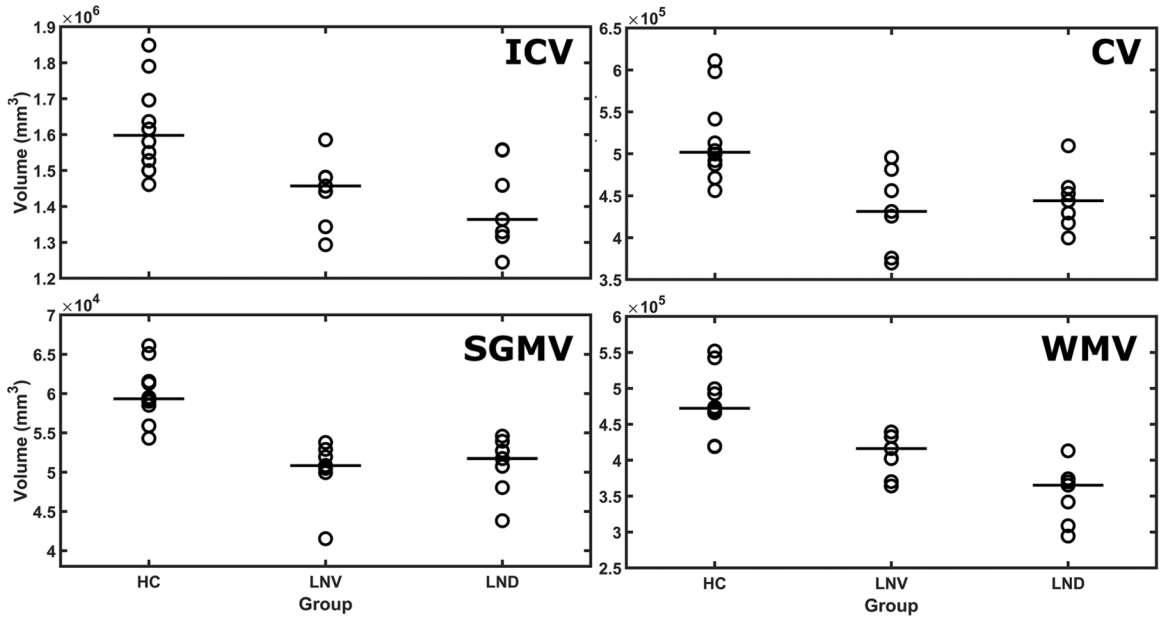

FIGURE 1.

Median brain volumes by group. Median brain MRI volumes for total intracranial volume (ICV), cortical grey matter volume (CV), subcortical grey matter volume (SGMV) and white matter volume (WMV) are plotted. HC, healthy control; LND, Lesch–Nyhan disease; LNV, Lesch–Nyhan variant

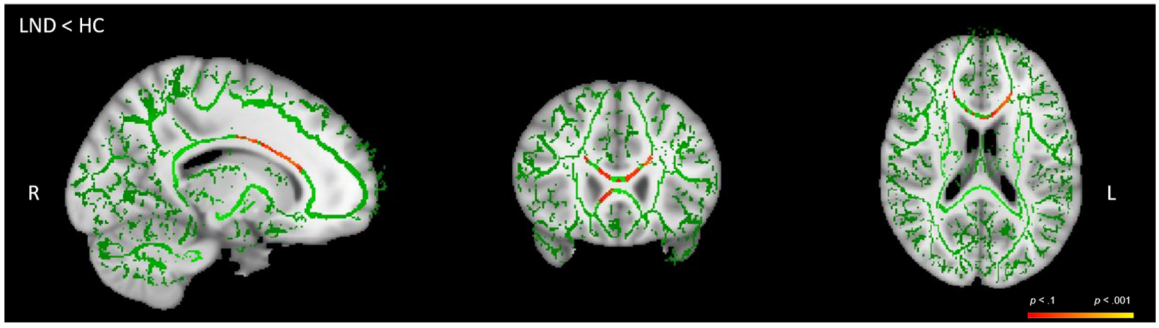

FIGURE 2.

Reduced fractional anisotropy (FA) in LND patients, (LND) < HC. Unthresholded tract-based spatial statistics (TBSS) results for (LND) < HC. Green is the skeleton, with shades of red and orange representing areas of white matter tracts of FA differences. HC, healthy control; LND, Lesch–Nyhan disease

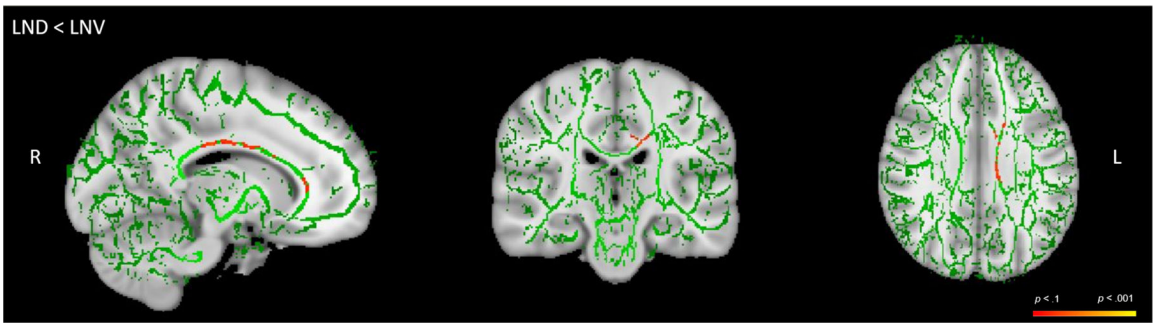

FIGURE 3.

Reduced fractional anisotropy (FA) in LND patients relative to LNV, LND < LNV. Unthresholded tract-based spatial statistics (TBSS) results for LND < LNV. Green is the skeleton, with shades of orange and red representing areas of white matter tracts of FA differences. HC, healthy control; LND, Lesch–Nyhan disease; LNV, Lesch–Nyhan variant

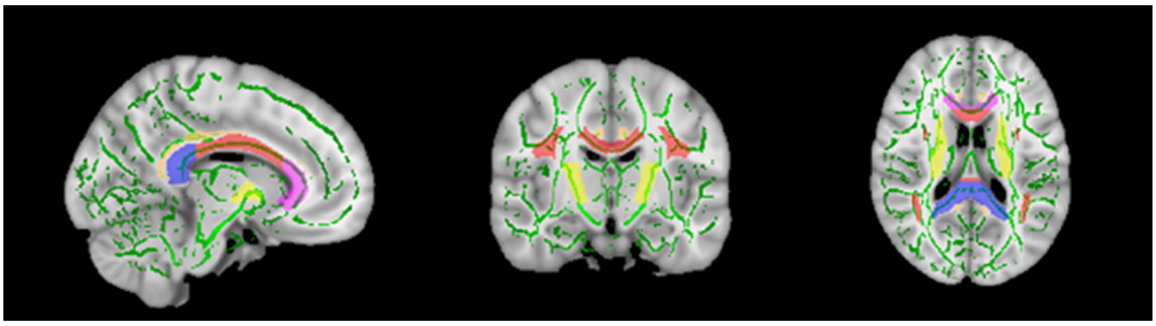

FIGURE 4.
Region of interests for fractional anisotropy (FA) maps. Map of the JHU DTI-based white-matter atlas that was used to extract regions of interest

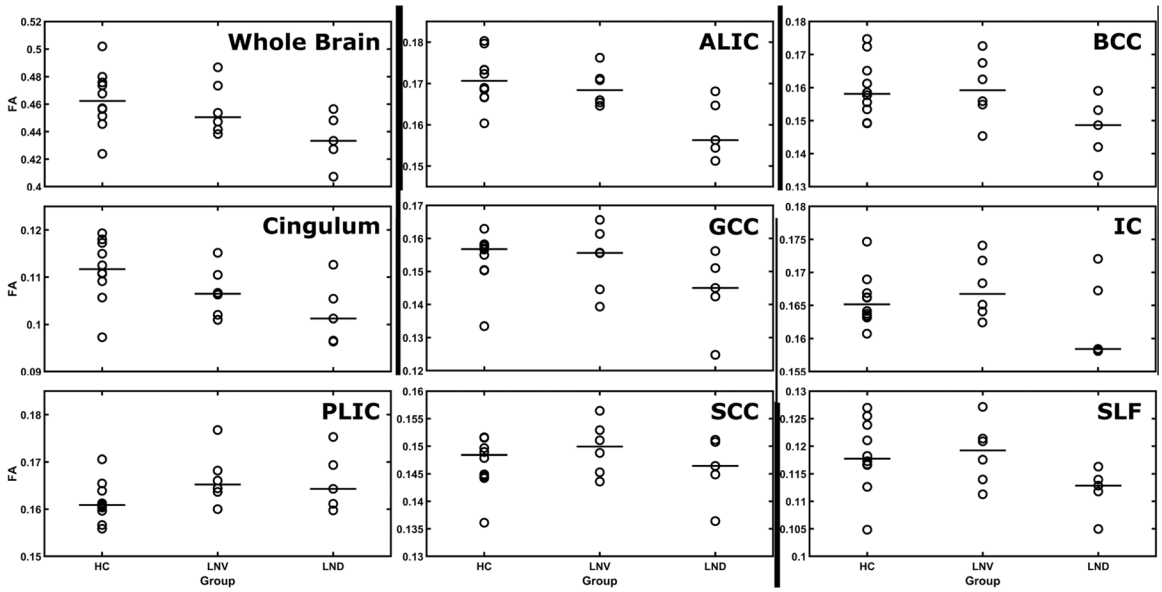

FIGURE 5.

Median fractional anisotropy (FA) values by group. Median FA values JHU DTI-based white-matter atlas for the following bilateral regions of interest: whole brain, cingulum, internal capsule (IC), anterior limb of the internal capsule (ALIC), posterior limb of the internal capsule (PLIC), genu of the corpus callosum (GCC), body of the corpus callosum (BCC), splenium of the corpus callosum (SCC) and the superior longitudinal fasciculus (SLF). HC, healthy control; LND, Lesch–Nyhan disease; LNV, Lesch–Nyhan variant

TABLE 1

Demographic, cognitive and clinical characteristics of participants

Group & ID #	Age	Race	HVLT-R learning	HVLT-R delay	BTA	IQ	BFRT	BFM
LND 1	19	White	14	3	2	69	14	44.5
LND 2	35	White	9	0	8	65	13	90
LND 3	30	White	16	8	5	72	24	63
LND 4	16	White	7	3	0	59	20	59
LND 5	30	Black	10	3	0	44	10	96
LND 6	45	White	9	1	1	51	14	86.5
LND 7	19	White	2	0	0	41	13	67.5
LNV 1	23	White	15	3	4	72	15	61.5
LNV 2	50	White	27	5	9	66	21	2
LNV 3	28	White	21	7	7	67	17	6
LNV 4	33	White	16	6	4	64	18	47.5
LNV 5	42	White	19	7	8	84	20	13.5
LNV 6	68	White	10	4	6	69	19	12.5
LNV 7	45	Black	6	1	1	42	9	56.5
HC 1	26	White	36	12	20	–	–	–
HC 2	61	White	25	11	16	–	–	–
HC 3	16	White	30	10	18	87	19	0
HC 4	52	White	34	12	19	116	26	3
HC 5	52	White	25	11	20	–	–	–
HC 6	47	Black	22	7	20	101	24	0
HC 7	33	White	28	9	20	104	25	0
HC 8	48	White	28	8	16	–	–	–
HC 9	18	White	24	9	18	113	23	1
HC 10	25	Hispanic	24	4	19	122	25	0

Note: Results shown as raw scores except for IQ, shown as standard scores ($M = 100$, $SD = 15$). IQ based on Kaufman Brief Intelligence Test–Second Edition. Abbreviations: BFM, Burke–Fahn–Marsden Dystonia Rating Scale; BFRT, Benton Facial Recognition Test; BTA, Brief Test of Attention; HC, healthy control; HVLT-R delay, Hopkins Verbal Learning Test–Revised delayed recall; HVLT-R learning, Hopkins Verbal Learning Test–Revised total learning over trials 1–3; LND, Lesch–Nyhan disease; LNV, Lesch-Nyhan variant.

TABLE 2

Demographic and MRI volumetric values per participant

	DTI	Brain volumes (mm^3)												
	WB FA	**ICV**	**WMV**	**CV**	**SGMV**	**Thal.**	**VD**	**Caud**	**Put**	**NA**	**Pall.**	**Hipp.**	**Amyg.**	**Cerebell.**
LND														
LND 1	0.245	1.56E+06	3.09E+05	4.17E+05	5.39E+04	14,615.5	8709.3	5969.3	8121.8	721.3	3488.1	7082.0	3415.5	144,230.1
LND 2	0.242	1.56E+06	4.13E+05	4.44E+05	5.27E+04	13,023.0	7261.6	5478.4	8899.2	865.3	3709.2	7985.5	3504.3	124,413.8
LND 3	0.252	1.46E+06	3.70E+05	4.53E+05	4.80E+04	11,085.9	6818.2	4440.3	8253.6	848.3	3387.3	8287.9	3498.8	120,683.3
LND 4	0.249	1.36E+06	3.65E+05	5.09E+05	5.46E+04	12,847.6	7611.4	7221.9	9747.7	858.1	3613.1	7980.8	3115.6	136,909.3
LND 5	0.258	1.33E+06	3.74E+05	4.29E+05	5.17E+04	13,607.2	7317.2	5709.9	8382.5	1266.5	3256.7	7044.6	3248.1	121,938.3
LND 6	0.248	1.32E+06	3.42E+05	4.00E+05	4.38E+04	10,190.9	6235.9	5259.7	7372.2	757.0	2715.7	7083.5	2692.2	118,712.5
LND 7	0.246	1.24E+06	2.94E+05	4.60E+05	5.08E+04	11,807.4	6964.3	6036.7	9272.3	944.2	3210.0	7900.4	3406.9	118,942.2
LNV														
LNV 1	0.267	1.59E+06	4.39E+05	4.81E+05	5.08E+04	12,113.3	6778.4	6526.9	8581.8	1399.0	3624.3	7474.2	2820.1	127,198.6
LNV 2	0.256	1.48E+06	4.17E+05	4.56E+05	4.99E+04	11,796.3	7020.9	5955.5	8621.3	1034.1	3553.3	7230.9	3255.7	109,110.9
LNV 3	0.277	1.48E+06	4.16E+05	4.96E+05	5.19E+04	13,387.4	7550.0	4874.1	9008.0	1059.1	3223.0	8232.8	3090.1	104,808.9
LNV 4	0.269	1.46E+06	4.02E+05	4.31E+05	5.38E+04	12,211.9	8543.9	5607.9	8944.1	1102.7	3638.2	8277.6	3893.2	139,666.7
LNV 5	0.246	1.44E+06	4.33E+05	4.26E+05	5.05E+04	11,696.4	6726.3	5184.9	8804.8	1004.9	3238.1	8522.4	3733.2	128,421.8
LNV 6	0.243	1.34E+06	3.70E+05	3.76E+05	4.15E+04	9582.6	6395.3	5178.0	6788.5	672.0	2522.9	6635.5	2468.4	117,823.5
LNV 7	0.264	1.29E+06	3.64E+05	3.70E+05	5.29E+04	12,457.0	7181.0	5796.9	9572.2	1039.6	4036.1	8042.5	3243.5	119,020.8
HC														
HC 1	0.294	1.85E+06	5.52E+05	5.98E+05	6.61E+04	17,155.1	9246.0	8845.9	10,600.3	1432.7	4091.5	9295.7	3740.3	166,686.0
HC 2	0.261	1.79E+06	5.42E+05	5.13E+05	6.16E+04	14,861.5	8123.4	8261.2	11,074.7	1093.0	4113.3	8791.6	3431.0	142,263.9
HC 3	0.264	1.70E+06	4.68E+05	6.11E+05	6.51E+04	15,518.4	8949.9	7522.1	11,343.4	1947.9	3528.6	9882.6	4311.7	143,280.0
HC 4	0.279	1.64E+06	4.99E+05	4.87E+05	5.95E+04	14,105.4	8736.8	6893.3	8962.7	1263.3	3613.5	10,256.4	3993.3	151,008.0
HC 5	0.302	1.62E+06	4.93E+05	4.92E+05	5.92E+04	15,550.0	8335.0	6319.6	9478.2	1435.0	3686.1	9190.1	3530.4	153,840.5
HC 6	0.253	1.58E+06	4.71E+05	5.00E+05	6.13E+04	12,670.4	8025.9	6712.9	12,322.3	1163.5	4365.4	9391.7	4367.2	123,429.5
HC 7	0.286	1.55E+06	4.66E+05	5.04E+05	5.85E+04	14,108.7	8742.8	6445.8	10,344.2	1194.6	3579.2	8694.3	3772.8	154,673.4
HC 8	0.277	1.53E+06	4.74E+05	4.71E+05	5.59E+04	14,278.0	8757.9	6152.4	9168.4	1178.6	3989.7	7920.0	3094.5	133,473.5
HC 9	0.267	1.50E+06	4.20E+05	5.41E+05	5.90E+04	14,872.6	7591.5	7055.5	10,261.0	1373.1	3517.8	8798.2	3775.5	141,773.3
HC 10	0.270	1.46E+06	4.19E+05	4.56E+05	5.43E+04	13,374.8	7482.0	6473.6	10,127.0	1253.9	3802.3	7316.4	3099.9	128,281.8

Note: ICV, WMV, CV and SCV are expressed in scientific notation.

Abbreviations: Amyg., amygdala; Caud., caudate nucleus; Cerebell., cerebellum; CV, cortical volume; HC, healthy control; Hipp., hippocampus; ICV, total intracranial volume; LND, Lesch–Nyhan disease; LNV, Lesch–Nyhan variant; NA, nucleus accumbens; Pall., pallidum; Put., putamen; SGMV, subcortical grey matter volume; Thal., thalamus; VD, ventral diencephalon; WMV, white matter volume.

TABLE 3

Hedges *g* effect size differences between groups

	Brain volume				Cognitive/Clinical measures					
	ICV	**WMV**	**CV**	**SGMV**	**HVLT IR**	**HVLT DR**	**BTA**	**KBIT2**	**BFRT**	**BFM**
LND vs. LNV	0.31	1.41	−0.24	−0.14	1.07	0.80	1.05	0.68	0.33	−1.83
LND vs. HC	1.65	2.83	1.51	2.37	3.74	2.45	6.71	3.81[a]	2.16[a]	−5.68[a]
LNV vs. HC	1.49	1.82	1.58	2.44	1.90	1.82	5.80	3.09[a]	1.97[a]	−1.63[a]

Abbreviations: BFM, Burke–Fahn–Marsden Dystonia Rating Scale; BFRT, Benton Facial Recognition Test; BTA, Brief Test of Attention; CV, cortical volume; HVLT DR, Hopkins Verbal Learning Test delayed recall; HVLT IR, Hopkins Verbal Learning Test immediate recall; ICV, total intracranial volume; KBIT2, Kaufman Brief Intelligence Test Second Edition; SGMV, subcortical grey matter volume; WMV, white matter volume.

[a]Effect size calculations uses only the six healthy controls with data for the comparison. Effect size changes are in reference to the first group in the comparison such that positive values represent increases compared with the first group and negative values represent decreases from the first group.

TABLE 4

Mean FA differences between the HC and LND participants

	Coordinates				
Cluster Size[a]	***x***	***y***	***z***	***p*** ***a***[b]	**White matter regions**[c]
1814	105	151	91	$p = .057$	Bilateral genu of the CC, bilateral body of the CC and bilateral anterior corona radiata.

Abbreviations: FA, fractional anisotropy; HC, healthy control; LND, Lesch–Nyhan disease.

[a]Cluster size is measured in voxels.

[b]Alpha is FWE-corrected.

[c]CC, corpus callosum. Given the sample size, only 3003 permutations were calculated.

Eur J Neurosci. Author manuscript; available in PMC 2023 January 01.

TABLE 5

Mean FA differences between LND and LNV participants

	Coordinates				
Cluster Size[a]	*x*	*y*	*z*	*p* *a* [b]	White matter regions[c]
1809	103	104	102	$p = .054$	Left body, genu, and splenium of the CC; left cingulum; and left superior corona radiata

Abbreviations: FA, fractional anisotropy; LND, Lesch–Nyhan disease; LNV, Lesch–Nyhan variant.

[a]Cluster size is measured in voxels.

[b]Alpha is FWE-corrected. Starting with the most conservative threshold, each progressive *p* value describes new regions that are significant at the new threshold.

[c]CC, corpus callosum. Given small sample sizes, only 462 permutations were calculated.

TABLE 6

Hedges *g* effect size differences between groups for whole brain and regions of interest (ROI) fractional anisotropy (FA)

	Whole brain	Cingulum	IC	ALIC	PLIC	GCC	BCC	SCC	SLF
HC > Patients	0.65	1.18	0.09	0.67	−0.54	0.48	0.59	−0.03	0.58
HC > LND	1.14	1.31	0.48	0.95	−0.18	1.21	1.44	0.50	1.10
HC > LNV	0.19	1.13	−0.39	0.25	−0.77	−0.22	−0.02	−0.84	0.11
LNV > LND	1.32	0.93	0.76	1.33	0.16	1.71	1.89	1.09	1.10

Note: All values have been adjusted for age and scan sequence/software used. Positive values indicate the first reference group is greater.

Abbreviations: ALIC, anterior limb of the internal capsule; BCC, body of the corpus callosum; IC, internal capsule; GCC, genu of the corpus callosum; HC, healthy control; LND, Lesch–Nyhan disease; LNV, Lesch–Nyhan variant; PLIC, posterior limb of the internal capsule; SCC, splenium of the corpus callosum; SLF, superior longitudinal fasciculus.